Reactivity of vanadyl pyrophosphate catalyst in ethanol ammoxidation and β-picoline oxidation: Advantages and limitations of bi-functionality

Reactivity of Vanadyl pyrophosphate catalyst in ethanol ammoxidation and β-picoline oxidation: advantages and limitations of bi-functionality

Tommaso Tabanelli, Massimiliano Mari, Federico Folco, Federico Tanganelli, Francesco Puzzo, Laura Setti, Fabrizio Cavani

Dipartimento di Chimica Industriale "Toso Montanari", Università di Bologna, Viale del Risorgimento 4, 40136 Bologna, Italy.

E-mail: fabrizio.cavani@unibo.it.

Dipartimento di Chimica Industriale "Toso Montanari", Alma Mater Studiorum Università di Bologna, Viale Risorgimento 4, 40136 Bologna, Italy

Keywords: Vanadyl pyrophosphate, ethanol, ammoxidation, acetonitrile, β-picoline, oxidation, nicotinic acid, catalyst bi-functionality.

Abstract

This study investigates the catalytic activity of vanadyl pyrophosphate (VPP) for both gas-phase ethanol ammoxidation to acetonitrile and β-picoline oxidation to nicotinic acid. These two reactions are of interest to the chemical industry: nicotinic acid is an essential human nutrient, whereas acetonitrile is mainly used as a solvent. Both reactions may be alternative processes to the industrial technologies used to produce these two chemicals. The reaction networks were investigated, also by feeding possible intermediates; *in-situ* DRIFT spectroscopy was used to monitor the interaction of ethanol and ammonia with the VPP catalyst. VPP bi-functionality

features (redox and acid) played an important role in the two reactions; specifically, acidity was detrimental either because it catalyzed undesired reactions, such as ethanol dehydration to ethylene during ethanol ammoxidation, or because it caused a strong interaction with reactants – especially those containing N atoms, ammonia and β-picoline – thus giving rise to some surface saturation phenomena which inhibited the consecutive reactions leading to the final desired compounds, acetonitrile and nicotinic acid. The co-feeding of steam helped product desorption, thus enhancing selectivity in β-picoline oxidation.

1. Introduction

Multifunctionality in heterogeneous catalysts is a fundamental trait useful for performing complex transformations[1], and this is especially important in oxidation catalysts for the transformation of organic substrates [2,3]. One emblematic example is vanadyl pyrophosphate (VPP), one of the most successful multifunctional catalysts used for mild oxidation reactions [2,4–9]. In addition to being used in industry for the oxidation of *n*-butane to maleic anhydride [4,10–17], it also performs well in other reactions, such as the oxidation of *n*-pentane to maleic and phthalic anhydrides [18–24], the oxidation of propane [25–28], and the ammoxidation of alkylaromatics [29–34], but also in liquid-phase reactions with H_2O_2 or alkylhydroperoxides for the oxidation of various organic substrates (*p*-cymene, cyclohexane) [35–39]. Some recent applications take advantage of its intrinsic bifunctional (both acid and redox) properties, such as the oxidative dehydration of glycerol to acrylic acid [40–44] and of 1-butanol to maleic anhydride [45]. Also in the case of oxidation reactions, surface acidity is believed to play an important role in the reaction mechanism [46–51]. Indeed, this catalyst has also been used for reactions which require acid sites only [40,41,52].

With the aim of finding new applications for the VPP catalyst, we investigated its behavior in two different gas-phase reactions, namely the ammoxidation of ethanol to acetonitrile and the oxidation of β-picoline to nicotinic acid (Scheme 1a and 1b, respectively).

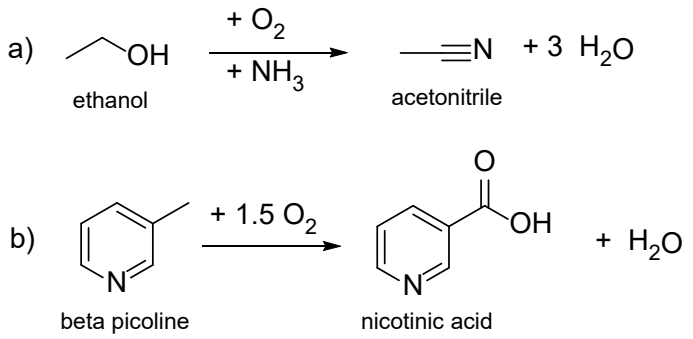

Scheme 1. Ethanol ammoxidation to acetonitrile (a) and β-picoline oxidation to nicotinic acid (b).

In the case of ethanol ammoxidation, the choice of VPP was based on the fact that, in literature, a catalyst made of vanadium oxide and phosphate is considered to be one of the systems offering the best selectivity and yield to acetonitrile in ethanol ammoxidation, even though the presence of the VPP structure is not explicitly reported in those papers [53,54]. Moreover, VPP has also been investigated as a catalyst for the direct gas-phase ammoxidation of alkylaromatics into the corresponding nitriles [33,55,56]. In this reaction, acidity might either play the detrimental role of catalyzing the undesired parallel reaction of ethanol dehydration to ethylene or, conversely, facilitate the desired reaction by the dehydration of the intermediately formed hemiaminal compound (1-aminoethanol CH_3-CH(OH)-NH_2). The latter is obtained by adding ammonia to the carbonyl moiety in acetaldehyde, the product of ethanol dehydrogenation; in fact, the hemiaminal may be the precursor of either acetaldehyde imine (ethanimine, via dehydration), or acetamide (via dehydrogenation or oxidative dehydrogenation), where imine is the precursor of acetonitrile [57–60]. We recently reported on the ammoxidation of ethanol using supported vanadium oxide

catalysts; the characteristics of the support were found to play an important role in the catalytic behavior [61–63].

As for the oxidation of β-picoline to nicotinic acid, the reaction has been thoroughly investigated over the past 20 years [64–94]; it is reported to be catalyzed by anatase-supported V_2O_5, but acidity (tunable by controlling the sulphate content in the support) plays a key role in helping the desorption of the acid, and hence contributes to achieving a selective process [83,84].

The two reactions examined are of interest to the chemical industry. Nicotinic acid is an important molecule, also known as niacin or vitamin B3, an essential human nutrient [68,89]. Ethanol ammoxidation might provide an alternative synthetic pathway for the production of acetonitrile from a bio-based building block, while today acetonitrile is obtained mainly as a by-product of propylene ammoxidation to acrylonitrile [95–98].

2. Experimental

The equilibrated VPP supplied by DuPont was used for catalytic experiments. The full characterization of this catalyst is reported in literature. [99] This catalyst was characterized by means of both X-ray powder diffraction (XRD) and single-point BET for the determination of a specific surface area.

A Philips PW 1710 apparatus, with Cu Kα (λ= 1.5406 Å) as radiation source in the range of $5°<2\theta<80°$, was used for XRD measurements. Reflections were attributed via the Bragg law, using the d value: $2d \sin \theta = n \lambda$. The XRD pattern of the equilibrated catalyst is shown in Figure S1.

The specific surface area (10±1 m^2/g in the case of the equilibrated VPP) was determined by N_2 absorption at 77K with a Sorpty 1750 Instrument (Carlo Erba). The sample was heated to 150°C,

under vacuum, to eliminate water and other molecules possibly adsorbed on the surface. After this pretreatment, the sample was maintained at 77K in a liquid nitrogen bath, while N_2 was adsorbed on the surface.

Catalytic experiments for ethanol ammoxidation were conducted as detailed in [61]. The reported W/F ratios refer to the loaded catalyst weight in the reactor divided by the volumetric flow rate and are generally expressed in $g*s*ml^{-1}$. Considering the toxicity of HCN, a by-product in the reaction, this compound was calibrated as follows: we conducted some experiments where HCN was formed, and performed both the online GC analysis and the titration with $AgNO_3$ of the aqueous basic solution obtained by bubbling the outlet stream in water. We found a linear relationship between the integrated area of the GC peak and the result of titration, thus making it possible for us to calculate a GC response factor for HCN.

Regarding the oxidation of β-picoline, catalytic tests were performed in a bench-scale apparatus. The glass reactor had a catalytic zone with a diameter of 12.7 mm and a porous quartz septum to hold the catalyst bed. A coaxial stainless-steel thermocouple holder was inserted from the top of the reactor to measure the temperature of the catalyst bed. Liquid reactants were fed by means of a syringe and an infusion pump (KDS scientific, KDS-100-CE) and then vaporized in an evaporator-mixing section, filled internally with quartz Raschig rings to achieve a better mix of vapors and gas. The heat necessary to vaporize liquid reactants was provided by a caulked resistance; also, the gas stream was pre-heated before being put in contact with the liquid stream. A cold trap was fitted at the end of the reactor; the trap was kept at a temperature of -20°C, to avoid the stripping of volatile liquid compounds such as pyridine and β-picoline. The flow containing gas-phase products was split into two streams – one sent directly to the vent, the other one to an on-line sampling for analysis – and lastly sent to the vent.

Reactant conversion and product yields were evaluated by means of gas-chromatography. The GC analysis was performed using an HP 5890 instrument equipped with a FID detector; helium was the carrier used. The acetone contained in the cold trap was added to other acetone used for the cleaning of the reactor bottom part, where condensation of heavy compounds may occur; then a precise quantity of the internal standard was added, and lastly the solution was analyzed. However, carboxylic acids were esterified prior to injection, because their GC-analysis is typically difficult. A DB-5ms column was used, which provided a good separation of the main products, but with a partial overlap of 3-pyridinecarbaldehyde and 3-piridinenitrile peaks. By tuning the carrier gas flow, however, it was possible to obtain a reasonable separation of the two peaks. The internal standard used was undecane. After the trap, the stream containing gaseous products, such as CO and CO_2, was conveyed to the on-line sampling system; the calibrated volume of gas was analyzed by means of a packed column 3m x 1/8" filled with Carbosieve SII (Supelco). Helium was the carrier gas, and a TCD was the detector.

The values of conversion, yield and selectivity to products were determined using the following equations:

$$Conversion = \frac{moles\ of\ converted\ reactant}{moles\ of\ fed\ reactant} \times 100$$

$$Yield_{product\ x} = \frac{moles\ of\ generated\ product_x \times\ number\ of\ C\ atom_{product\ x}}{moles\ of\ fed\ reactant \times\ number\ of\ C\ atom_{reactant}} \times 100$$

$$Selectivity_{product\ x} = \frac{Yield_{product\ x}}{Conversion} \times 100$$

$$C\ balance = \frac{\sum Yields}{Conversion}\ \mathrm{X}\ 100$$

Raman spectra were recorded using a Renishaw Raman System RM1000 instrument, equipped with a Leica DLML confocal microscope, with 5x, 20x, and 50x objectives, video camera, CCD

detector, and laser source Argon ion (514 nm) with a 25 mW power. The maximum spatial resolution was 0.5 μm and the spectral resolution 1 cm^{-1}. For each sample, several spectra were collected by changing the position of the laser beam. The parameters used for spectrum acquisition were: 5 accumulations, 10 seconds, 25% laser power to prevent damaging of the sample, and a 50x objective.

DRIFTS analyses were performed by pre-treating the sample at 500°C in a He flow (10 mL min^{-1}) for 60 min, in order to remove the molecules adsorbed. Then the sample was cooled down to the adsorption temperature (100°C) and a diluted NH_3 (10% NH_3 in He) was fed. Subsequently, He was left to flow until the weakly adsorbed ammonia was evacuated. In the case of TPD experiments, the temperature was raised up to 350°C while spectra were recorded every 50°C. Ethanol was pulsed at 350°C and spectra were taken for 60 minutes. The IR apparatus used was a Bruker Vertex 70 equipped with a Pike DiffusIR cell. Spectra were recorded using an MCT detector after 128 scans and a 2 cm^{-1} resolution. The mass spectrometer was an EcoSys-P from European Spectrometry Systems.

TPD/MS experiments were conducted using the Micromeritcs Autochem II instrument equipped with a MKS Cirrus detector. Before experiments, the sample was pre-treated at 350°C in He flow, in order to clean the surface from the molecules adsorbed. The adsorption was conducted at 100°C by pulsing NH_3 (10% NH_3 in He). Desorption was conducted by feeding pure He or He with 5% O_2, while heating the sample from 100°C up to 650°C. A part of the outlet gas was sent to the mass spectrum detector.

3. Results and Discussion

3.1 Ethanol ammoxidation to acetonitrile: the reaction network

We first conducted some experiments by feeding the reactant mixture without any catalyst, and by filling the reactor with inert material (corundum). We found that ethanol conversion ranged between 3 and 8% in the temperature interval 300 to 500°C; the main product was acetaldehyde, with a minor formation of CO and CO_2. This means that the contribution of both wall-catalyzed and homogeneous reactions was small, and can be disregarded during catalytic experiments.

Figure 1 shows the results of ethanol ammoxidation using a feed composition consisting of 5 mol% ethanol (azeotropic composition), 13 mol% oxygen, 13 mol% ammonia, and the remainder inert. In all experiments, we typically used He as the ballast component, because this permitted a better analysis of the N_2 produced during the reaction; worthy of note, the use of N_2 or Ar produced the same results as with He.

The results shown in Figure 1 demonstrate that the catalyst was moderately selective to acetonitrile; the total conversion of ethanol was reached at around 440°C, for a W/F ratio of 0.80-0.85 g s ml^{-1}; both ammonia and oxygen conversion reached the maximum value of 35-40% at high temperature, these reactants being fed in excess with respect to the stoichiometric amount required for acetonitrile synthesis. At low temperature, acetaldehyde was the main by-product, whereas selectivity to $CO+CO_2$, ethylene and HCN were no higher than 10% at 350°C. The temperature increase, however, led to a progressive decline in selectivity to both acetaldehyde and acetonitrile, and to a rapid rise in selectivity to ethylene and to $CO+CO_2$; selectivity to HCN was not much affected by temperature.

Figure 1 also shows the selectivity to “heavy compounds”, which were calculated considering the C balance; these compounds were in part eluted in the GC column (but were not identified, being in a very small amount), and in part accumulated over the catalyst. Nevertheless, their relative amount was low, if compared to the corresponding amount formed at a greater ethanol

concentration (see below). One additional important effect observed was the rise in selectivity to N_2, deriving from ammonia combustion.

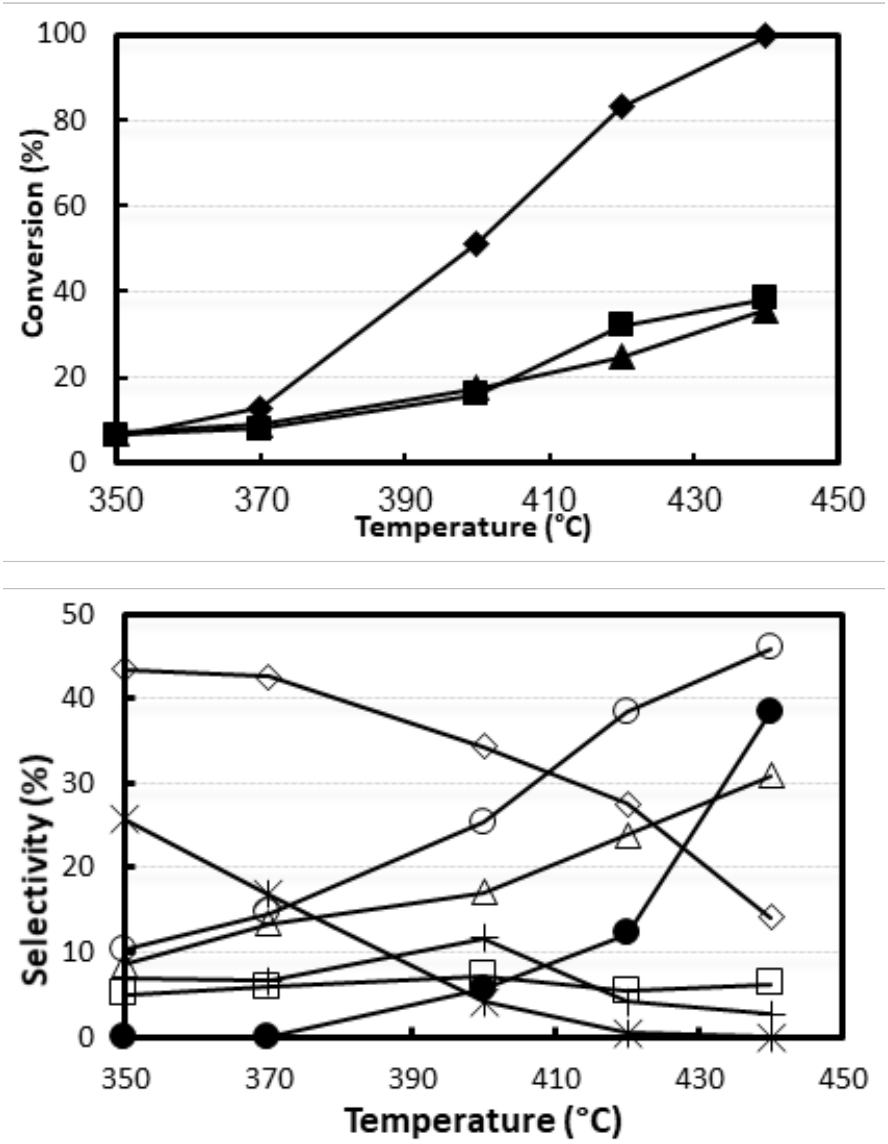

Figure 1. Effect of temperature on reactant conversion (top figure) and selectivity to products (bottom figure). Reaction conditions: W/F ratio 0.8 g s ml^{-1}, feed composition (molar %): ethanol (azeotrope ethanol/water 95.6/4.4 wt%)/ammonia/oxygen/inert 5/13/13/69. Symbols: ethanol conversion (◆), ammonia conversion (▲) and oxygen conversion (■). Selectivity: acetonitrile (◇), acetaldehyde (∗), ethylene (△), $CO+CO_2$ (○), HCN (□), heavy compounds (+) and N_2 (calculated with respect to converted ammonia) (●). Catalyst VPP.

The results reported demonstrate that the distribution of products was greatly affected by reaction conditions; the low selectivity to acetonitrile derived from the contribution of both parallel reactions: one leading to ethylene, HCN and $CO+CO_2$, and a consecutive one leading to carbon oxides. Therefore, an efficient transformation of acetaldehyde into acetonitrile is an important requisite when aiming to achieve a high selectivity to nitrile.

To confirm the role of acetaldehyde as the key reaction intermediate in the sequence of reactions leading to the formation of acetonitrile, we conducted experiments in which we changed the W/F ratio, at fixed temperature (370°C and 440°C) and feed composition (ethanol/ammonia/oxygen 5/13/13, mol%); the results are shown in Figures 2 and S2.

At 370°C (Figure 2), reactant conversion was lower than 15%. As for the distribution of products in function of the W/F ratio, our results indicate that the only primary products were ethylene and acetaldehyde; the selectivity to ethylene then underwent only a minor decrease when the W/F ratio was increased, whereas that to acetaldehyde rapidly declined, with a corresponding increase in selectivity to acetonitrile, $CO+CO_2$, HCN, and some undetected heavier compounds as well; however, the selectivity to the latter products reached a maximum value at 0.2 g s ml^{-1} W/F ratio and then declined.

These experiments confirm the kinetic relationship between acetaldehyde and acetonitrile, suggesting that this mechanism occurs by the reaction of aldehyde with ammonia and the generation of the ethanimine intermediate compound. Furthermore, our data clearly highlight that the catalyst acidity is detrimental for catalytic behavior, since ethylene formation is already significant at 370°C. In this case, the formation of N_2, deriving from ammonia combustion, was negligible, because of the low temperature used.

When our experiments were conducted at 440°C (Figure S2), the same reaction network was inferred, with acetaldehyde and ethylene as the only primary products. It is worth noting that the initial selectivity to $CO+CO_2$ (i.e. the selectivity extrapolated to nil conversion) was close to zero; this means that ethanol did not undergo a direct reaction of combustion even at such a relatively high temperature. Once again, the rapid decline in acetaldehyde selectivity corresponds to the increased selectivity to acetonitrile, HCN, $CO+CO_2$ and heavy compounds.

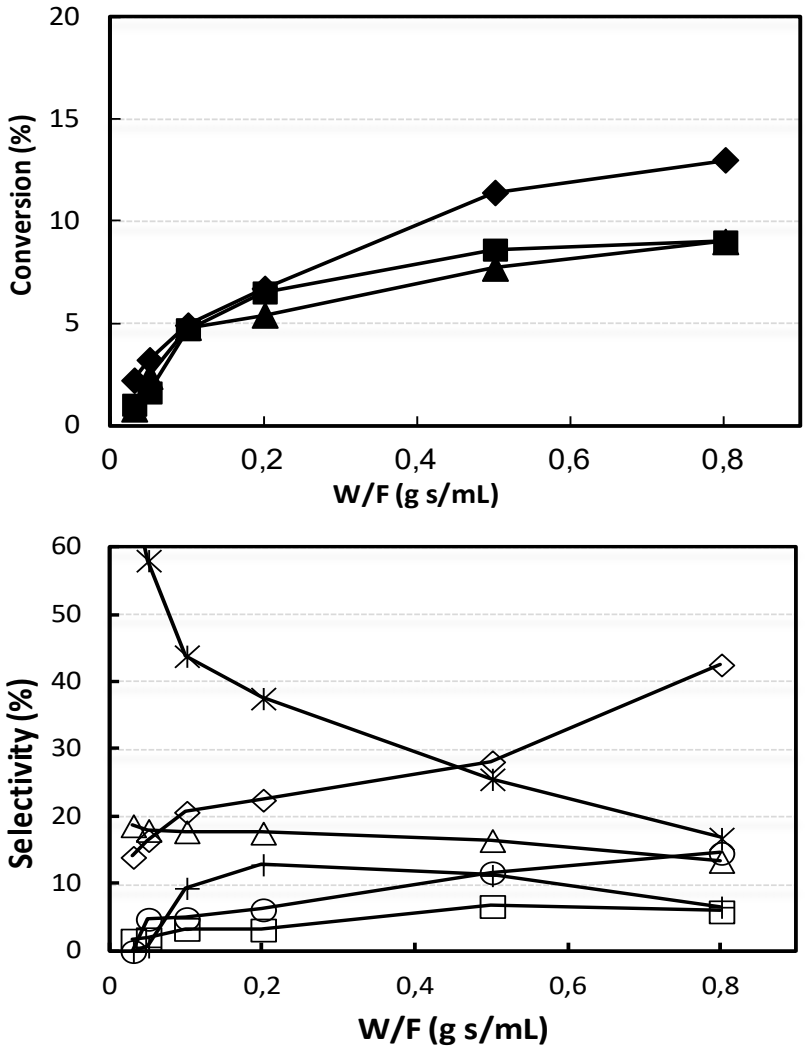

Figure 2. Effect of W/F ratio on reactant conversion (top figure) and on selectivity to products (bottom figure). Reaction conditions: T 370°C, feed composition (molar %): ethanol (azeotrope)/ammonia/oxygen/inert 5/13/13/69. Symbols: ethanol conversion (◆), ammonia

conversion (▲) and oxygen conversion (■). Selectivity to: acetonitrile (◇), acetaldehyde (∗), ethylene (△), $CO+CO_2$ (○), HCN (□), and heavy compounds (+). Catalyst VPP.

One major difference with respect to experiments conducted at a lower temperature is that at a W/F ratio above 0.1-0.2 g s ml^{-1}, the selectivity to both acetonitrile and heavy compounds decreased. Therefore, at high temperature, acetonitrile is not a stable compound and undergoes consecutive oxidation to CO_x.

These experiments demonstrate that the relatively low selectivity obtained with the VPP catalyst is related not only to the important parallel contribution of ethanol dehydration into ethylene, but also to the fact that the key reaction intermediate undergoes consecutive transformations to both the desired compound and its by-products – i.e. CO, CO_2, and HCN – and to heavy compounds as well. Lastly, even acetonitrile undergoes consecutive combustions when the reaction is conducted at high temperature.

3.2 Ethanol ammoxidation to acetonitrile: the role of reactant partial pressure

The control of selectivity in partial oxidation reactions, when conducted with mixed oxide catalysts (and especially with the VPP), is closely related to the redox properties of the active metal ion and its average oxidation state under steady conditions, the latter being affected in turn by the gas-phase composition. Therefore, we conducted a series of experiments in which we changed the partial pressure of ethanol, while keeping the inlet concentration of oxygen and ammonia constant; ethanol molar fractions equal to 0.02, 0.05, 0.075 and 0.13 were used. Results are summarized in Figure 3. The following effects were noted:

a) The conversion of ethanol, which in all cases increased over the range of temperature examined, showed a decreasing trend in correspondence to an increased partial pressure of

ethanol in the feed. This is a clear indication of a surface saturation effect; in fact, the rank of the overall integral rate of ethanol transformation, measured at 400°C, was: 2.5% ethanol < 5% ethanol ≈ 7.5% ethanol ≈ 13% ethanol. An alternative explanation for the phenomenon observed is that under relatively high concentrations of ethanol and ammonia, when both compounds act as reducing species in the redox cycle, the catalyst evolves to a more reduced steady state, e.g. with predominance of V^{4+} as compared to V^{5+} sites. This implies that there is a decrease in the number of moles of reactants which may interact per unit time with the catalyst surface, whereas the number of oxygen moles increases. This basically corresponds to a surface saturation, observed at higher ethanol concentration.

b) The selectivity to acetonitrile showed either a maximum value at an intermediate temperature or continuously decreasing values; generally speaking, the decrease corresponded to an increased formation of $CO+CO_2$, whereas the presence of a maximum value was due to a relatively higher formation of undetected compounds ("heavy" compounds) at a lower temperature. The best selectivity was seen in the lowest concentrations of ethanol in the feed; the greater difference was seen when the concentration of ethanol was increased from 5% to 7.5%, and this was mainly due to the greater formation of heavy compounds.

c) The selectivity to acetaldehyde declined when the temperature was raised; the greatest selectivity was shown with tests conducted at the highest ethanol concentration. This may occur because, under conditions of surface saturation, the reactions involving acetaldehyde are slower than on a "clean" surface. Moreover, under these conditions acetaldehyde was less efficiently transformed into acetonitrile, and underwent side reactions to form heavier compounds.

d) The selectivity to ethylene was not much affected by ethanol partial pressure; this indicates that ethanol dehydration to ethylene occurred on sites which were different from those responsible for ethanol (oxi)dehydrogenation into acetaldehyde. In these sites also, however, a saturation effect was observed when ethanol concentration was raised, because the overall rate of ethylene formation reached a plateau.

e) In all experiments, the selectivity to $CO+CO_2$ increased in parallel with the temperature rise; however, the variation seen differed depending on the ethanol partial pressure. In fact, in experiments conducted using 2 and 5% ethanol in the feed, the selectivity to $CO+CO_2$ was relatively low at low temperature, but then the rise observed with an increase in temperature was very rapid. Conversely, in experiments conducted using 7.5 and 13% ethanol in the feed, the selectivity to $CO+CO_2$ was slightly higher at a lower temperature, compared to experiments at lower ethanol concentration, but then the increase seen in parallel with the temperature increase was not so significant. As a result, at high temperature and ethanol concentration, the selectivity to $CO+CO_2$ was much lower than that observed under leaner ethanol conditions. This effect can be explained by taking into account the surface saturation due to the adsorbed C_2 molecules. A saturation implies a lower availability of oxidizing sites (in other words, it can be considered a surface "over-reduction"), which are supposed to be responsible for the combustion to carbon oxides. Therefore, under these "saturated surface" conditions, the catalyst is less selective to combustion compounds, but more selective to heavier, condensation compounds.

f) The effect of ethanol concentration on the selectivity to N_2 was significant. The greater the ethanol concentration, the lower the amount of ammonia which was oxidized into molecular nitrogen. This is not just attributable to the fact that the reaction between the intermediately

formed acetaldehyde and ammonia was quicker compared to the parallel reaction of ammonia combustion when there was a greater concentration of adsorbed acetaldehyde. Indeed, an important contribution may derive, once again, from V over-reduction occurring under surface saturation conditions, which made the combustion of ammonia kinetically less significant than when the catalyst surface was cleaner.

In conclusion, a major outcome of these experiments is that the best yields to acetonitrile are obtained at either 2% (27% at 400°C and 22% at 420°C) or 5% ethanol in the feed (18% at 400°C and 23% at 420°C), but the best acetonitrile productivity was obtained with 5% ethanol in the feed, at 420°C. Therefore, further experiments were conducted using the feed composition of 5 vol% ethanol, 13% ammonia, and 13% oxygen (the conditions used for the experiments reported in Figures 1, 2, and S2).

Regarding the nature of the so-called "heavy" products, the following compounds were identified: fumaronitrile, pyrazine, lactonitrile, 2-ethylidenamino-propionitrile, and also some olefins, such as 3-methyl-1-butene and 2-pentene. The compounds formed in greater amounts were the products containing N; it is worth noting that they did not form by a consecutive reaction upon acetonitrile (which was a stable compound; see experiments reported below); therefore, we can assume that they formed starting from some N-containing intermediate, such as ethanimine. It is possible that the imine intermediate, which is very reactive, easily reacted under conditions of surface saturation with acetaldehyde or another adsorbed imine to generate condensation compounds, instead of being (oxi)dehydrogenated into the nitrile. It may be assumed that the relative rate between the two competitive reactions of acetaldehyde transformation (condensation vs. oxidehydrogenation) depended on both the concentration of adsorbed species and the availability of oxidizing V species

on the surface; the latter was lowest when the catalyst surface was completely covered by adsorbed intermediate compounds, acetaldehyde and ethanimine.

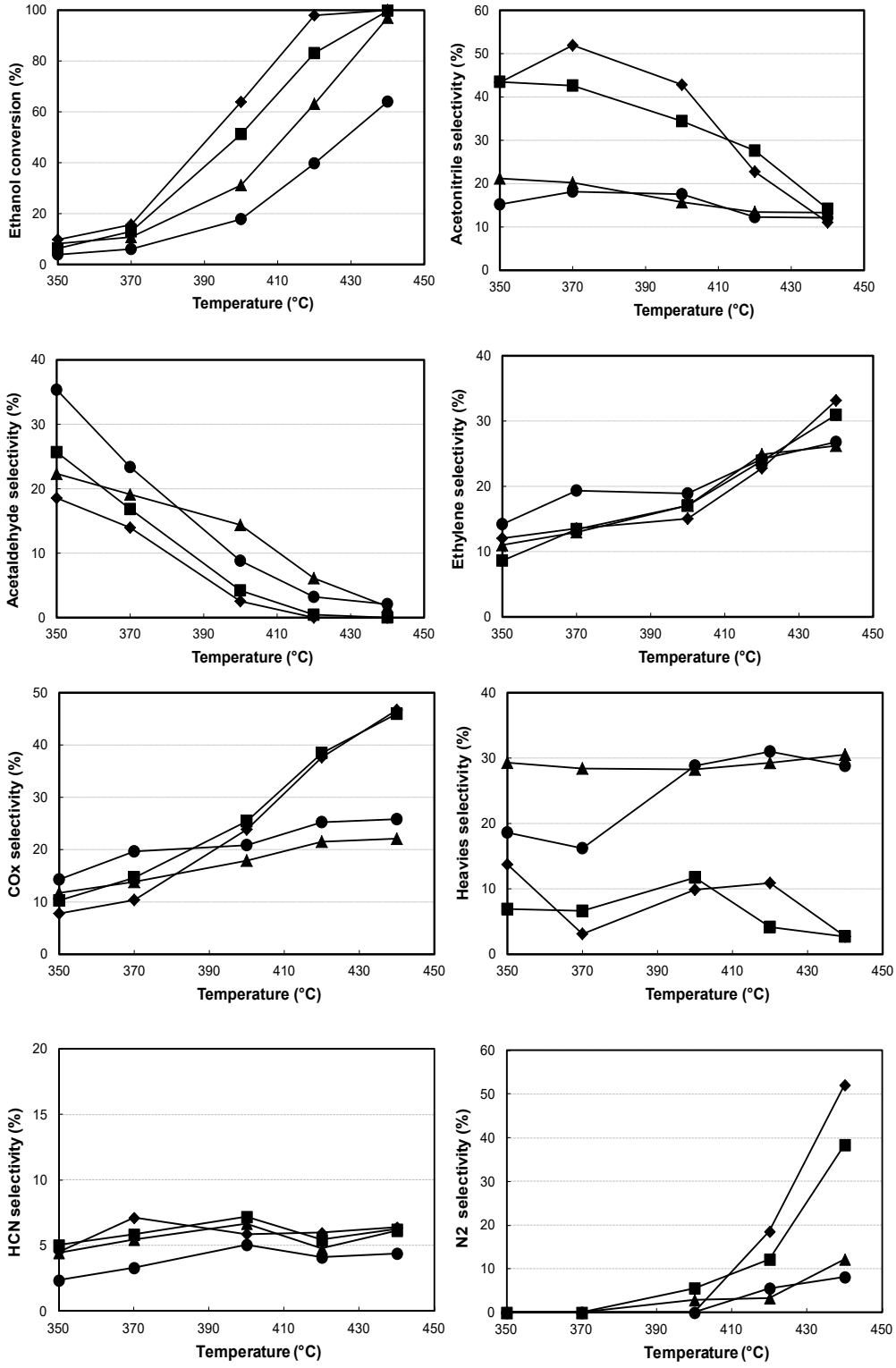

Figure 3. Conversion of ethanol, oxygen and ammonia, and selectivity to the products based on temperature. Feed composition: ethanol 2% (◆), 5% (■), 7.5 (▲), or 13% (●), ammonia 13%, oxygen 13%, remainder He. Catalyst VPP.

The data obtained based on W/F ratio at 440°C, using 7.5% ethanol in the feed – i.e. under conditions of surface saturation – confirm the hypothesis suggested. The results shown in Figure S3 demonstrate that the consecutive reaction occurring on acetaldehyde not only led to acetonitrile and $CO+CO_2$ (as also shown in the case of experiments conducted under non-saturated surface conditions), but also to heavy compounds. In fact, the selectivity to the latter increased in concomitance with the decrease of acetaldehyde. On the other hand, the selectivity to heavy compounds showed a peak, probably due to the consecutive combustion.

The effect of partial oxygen and ammonia pressures, at 0.8 g s ml^{-1} W/F ratio, 370°C, and with 5% ethanol in the feed, is shown in Figures 4 (ammonia 13%) and S4 (oxygen 13%), respectively. As for the effect of oxygen, it is shown that the increased partial pressure of oxygen led to a proportionally increased ethanol conversion; this means that (i) oxygen played an important role in the (oxi)dehydrogenation of ethanol to acetaldehyde (a primary product), and (ii) VPP does not catalyze the dehydrogenation of ethanol to the aldehyde.

Oxygen also affected the distribution of products considerably; it facilitated the transformation of acetaldehyde into CO, CO_2, and HCN, and into acetonitrile as well. This means that the formation of acetonitrile also involved the contribution of oxygen, for the oxidative dehydrogenation of ethanimine into the nitrile. On the other hand, concentrations of oxygen higher than 13% caused a decrease in the selectivity to acetonitrile, and a corresponding increased selectivity to CO_2. Oxygen did not affect the selectivity to ethylene, which is an expected result. The selectivity to heavy

compounds was below 10% over the entire range of oxygen partial pressures investigated, and it was not significantly affected by this parameter.

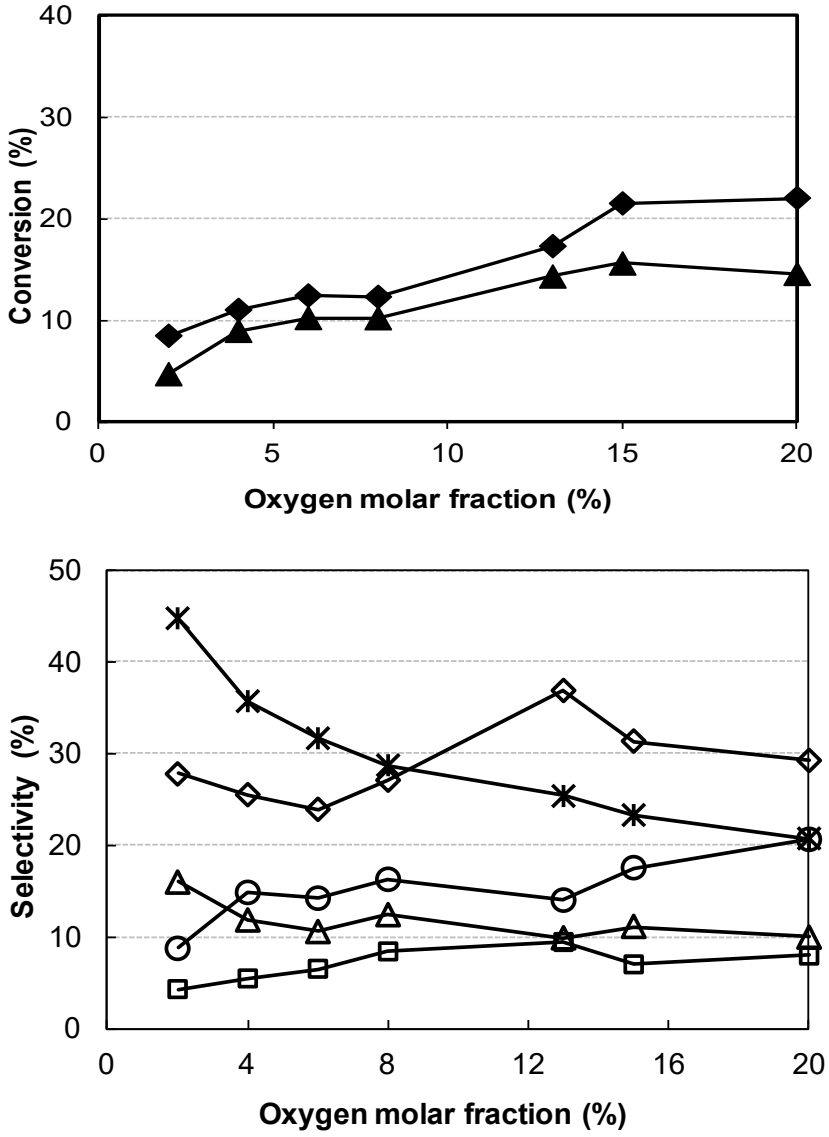

Figure 4. Effect of oxygen inlet molar fraction on reactant conversion (top figure) and selectivity to products (bottom figure). Reaction conditions: W/F ratio 0.8 g s ml^{-1}, T 370°C, feed composition (molar %): ethanol (azeotrope)/ammonia/oxygen/inert 5/13/x/82-x. Symbols: ethanol conversion (◆), and ammonia conversion (▲). Selectivity: acetonitrile (◇), acetaldehyde (✳), ethylene (△), $CO+CO_2$ (○), and HCN (□). Catalyst VPP.

As for the role of ammonia, Figure S4 shows that there is an inhibitory effect on ethanol conversion. This decrease is due to both a decline in yield to ethylene (in fact, the selectivity to this compound is not affected by ammonia), and in the rate for the reaction pathway leading to acetaldehyde and acetonitrile. Therefore, ammonia interacted with both types of sites, the acid one (leading to ethylene formation; this implies the existence of strong acid sites, which were poisoned by ammonia even at high temperatures), and of the redox one responsible for acetaldehyde formation.

3.3 Ethanol ammoxidation to acetonitrile: the reactivity of intermediates and products

With the aim of confirming the reaction mechanism suggested, we conducted experiments by feeding the possible reaction intermediates, acetaldehyde and ethylamine. In fact, even though experiments clearly highlighted the existence of a kinetic relationship between acetaldehyde and acetonitrile, we cannot rule out the possible existence of a side-reaction pathway, with a direct exchange between –OH and $–NH_2$; the amine might then yield acetonitrile by oxidehydrogenation.

$CH_3CH_2OH + NH_3 \leftrightarrows CH_3CH_2NH_2 + H_2O$

$CH_3CH_2NH_2 + O_2 \rightarrow CH_3CN + 2\ H_2O$

At first we conducted experiments by feeding acetaldehyde, with the following feed composition: acetaldehyde/ammonia/oxygen mol% 0.5/13/13; pure acetaldehyde was fed by means of vaporization, as we did with ethanol. We checked the effect of temperature (W/F ratio 0.8 g s ml^{-1}) and of W/F ratio (T 350°C); results are shown in Figures 5 and S5, respectively. We observed the following effects of temperature:

a) The C balance was very good, with no formation of heavy compounds; this was likely due to the low inlet concentration of the acetaldehyde used.

b) Acetaldehyde was very reactive; total conversion was already achieved at 400°C.

c) Aldehyde was mainly converted into acetonitrile and HCN, which formed with a similar selectivity; since selectivity referred to the number of C atoms, however, the number of HCN moles produced was greater than that of acetonitrile.

d) The $CO+CO_2$ selectivity trend was like that shown by HCN; however, the number of moles produced always remained smaller than that of HCN.

Overall, there are analogies but also differences in the behavior shown, compared to that observed with ethanol; the main difference concerns the large amount of HCN, which instead formed with low selectivity from ethanol, even at low ethanol concentration. Indeed, we would have expected a much more efficient transformation of acetaldehyde into acetonitrile, especially because of the very large amount of ammonia fed.

To interpret this difference, we conducted experiments based on the W/F ratio, at 350°C. The results reported in Figure S5 show that the main primary product of acetaldehyde transformation was acetonitrile. This, however, underwent consecutive transformations into both $CO+CO_2$ and, to a greater extent, HCN. After 0.8 g s ml^{-1} W/F ratio (which was the same used for the experiments reported in Figure 5), both acetonitrile and HCN underwent a consecutive transformation into CO_2 and N_2.

Therefore, these experiments made it possible for us to reach two important conclusions:

a) The scheme of the ethanol-to-acetonitrile reaction also includes the reactions of the consecutive transformation of acetonitrile into HCN and of both compounds into CO_2.

b) Since any consecutive reaction on acetonitrile and HCN was seen to contribute only marginally in the experiments conducted with ethanol at 370°C (Figure 2), we can conclude that these reactions were significant only under conditions of low surface saturation. In other

words, a non-saturated surface (because of the low acetaldehyde concentration fed during these experiments) was more active in the consecutive oxidative degradation of both acetonitrile (into HCN and $CO+CO_2$) and HCN (into CO_2 and N_2).

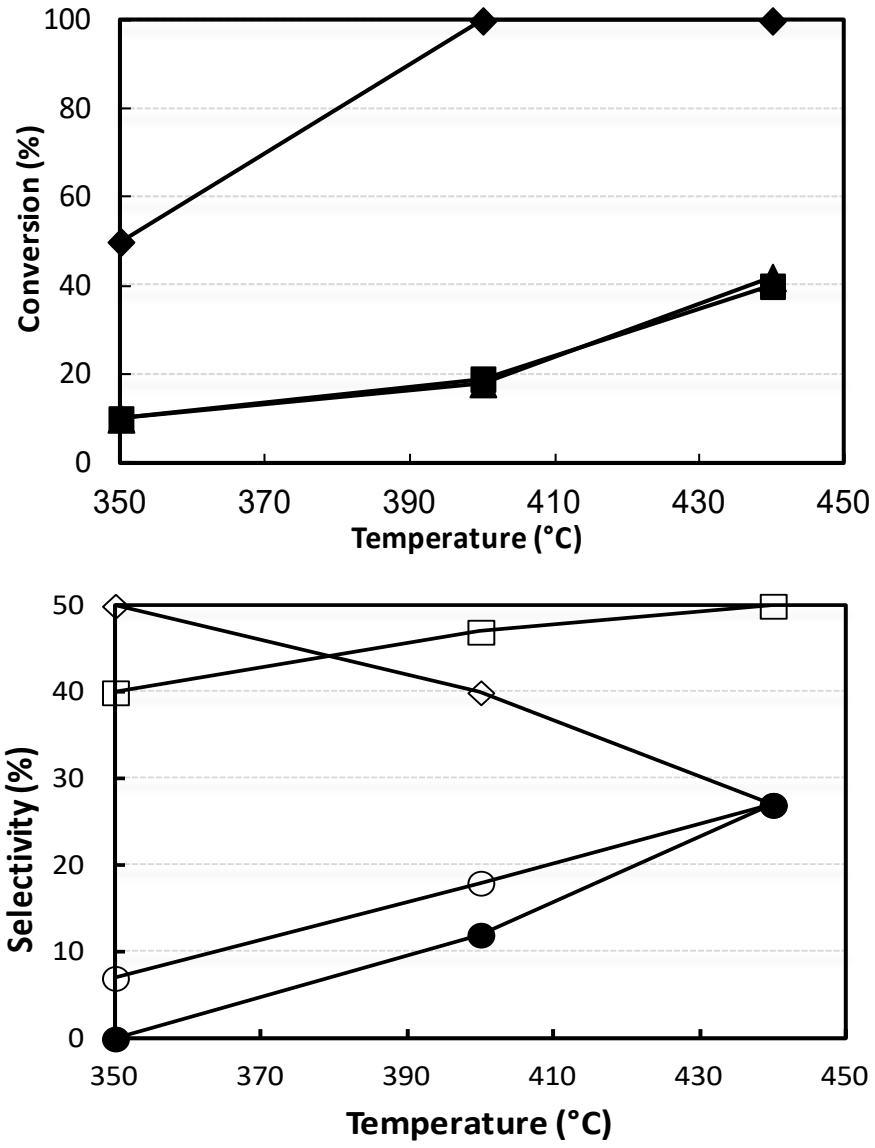

Figure 5. Effect of temperature on reactant conversion (top figure) and selectivity to products (bottom figure). Reaction conditions: W/F ratio 0.8 g s ml^{-1}, feed composition (molar %): acetaldehyde/ammonia/oxygen/inert 0.5/13/13/73.5. Symbols: acetaldehyde conversion (◆), ammonia conversion (▲) and oxygen conversion (■). Selectivity to: acetonitrile (◇), $CO+CO_2$ (○), HCN (□), and N_2 (calculated with respect to converted ammonia) (●). Catalyst VPP.

The presence of a non-saturated surface under the conditions used for these experiments was also demonstrated by the fact that there was practically no formation of heavy compounds. In order to confirm this hypothesis, we conducted some experiments by feeding 1.5% acetaldehyde (with 13% oxygen and 13% ammonia); because of the huge problems encountered with these experiments (formation of polymeric compounds, with blockage of reactor lines), we are unable to report on the values of the conversion and selectivity obtained. An important result, however, is that we observed the formation of large amounts of heavy compounds, which were exactly the same as those also formed in experiments with ethanol under surface saturation conditions: 2-ethylidene-amino-propionitrile, 1-butene-3 methyl, fumaronitrile, etc. Conversely, the only product not observed from ethanol was acetic acid; it formed, however, in a significant amount at 350°C, but in a negligible quantity at 400°C.

As for the reactivity of ethylamine, the results of the experiments conducted by feeding 0.9 mol% ethylamine and 13% oxygen are shown in Figure S6; these experiments were conducted without ammonia in the feed. The amine was very reactive; an almost total conversion was shown already at 350°C. Predominant products were carbon oxides, the selectivity of which was not affected by temperature, even though the CO/CO_2 ratio decreased, as also shown by the considerably increased oxygen conversion observed along with the temperature rise. The selectivity to acetonitrile was 20% at 350°C, but then it declined, with a correspondingly higher selectivity to HCN. At low temperature, we also observed the formation of small amounts of $CH_3CH_2N=C=O$. It is apparent that the low selectivity to ethylamine made it possible for us to disregard the reaction mechanism of acetonitrile formation via intermediate ethylamine formation.

Ethylene is one of the major by-products of the reaction from ethanol, and in all experiments conducted based on the W/F ratio, its selectivity was not affected by the latter parameter, thus

implying that it is a very stable product. This was confirmed by the experiments conducted by feeding ethylene, using the following feed composition: ethylene/ammonia/oxygen mol% 7.5/13/13. Results demonstrated that ethylene is poorly reactive, as shown by its modest conversion based on temperature (Figure S7). Minor products were HCN and COx, whereas the major product was tentatively attributed to toluene. This indicates that the VPP catalyst is able to transform olefin into aromatics, a property typically shown by acid catalysts.

The last issue investigated was the stability of acetonitrile under reaction conditions. In fact, experiments conducted based on the W/F ratio highlighted that acetonitrile is a rather stable product, at least under relatively mild conditions. We first conducted an experiment by feeding acetonitrile and oxygen, without a catalyst, in the temperature range 350-440°C; at 440°C, acetonitrile conversion was only 8%. This indicates that there is no homogeneous oxidative degradation of the product. Other experiments were conducted by feeding acetonitrile and oxygen with the VPP catalyst (Figure S8), using a low concentration of acetonitrile (1%) in order to simulate a cleaner and more oxidizing surface. Acetonitrile conversion was moderate, which confirms the relative stability of this compound, and the products observed were HCN and $CO+CO_2$; the former prevailed at high temperature, and the latter at low temperature. We also conducted experiments with a high concentration of acetonitrile in the feed (7.5%); in this case we observed the same products, but the C balance was very poor throughout the entire range of temperatures examined, due to the formation of heavy compounds (which instead formed in a smaller quantity during the experiments conducted with low acetonitrile concentration in the feed). In conclusion, the best acetonitrile yield achieved with the VPP catalyst was 27% only. This value was lower than in the compared literature data (as summarized in Table S1); this is probably due to several concomitant factors, such as (i) the intrinsic acidity, which leads to the formation of

ethylene, especially at the highest temperatures; (ii) the formation of heavy compounds, especially under conditions of surface saturation, also likely due to VPP surface acidity; (iii) the consecutive transformations of acetaldehyde, which originate the formation not only of acetonitrile, but also of carbon oxides; (iv) under specific conditions, the consecutive degradation of acetonitrile itself.

The reaction network, as inferred from the reactivity experiments, is summarized in Scheme 2.

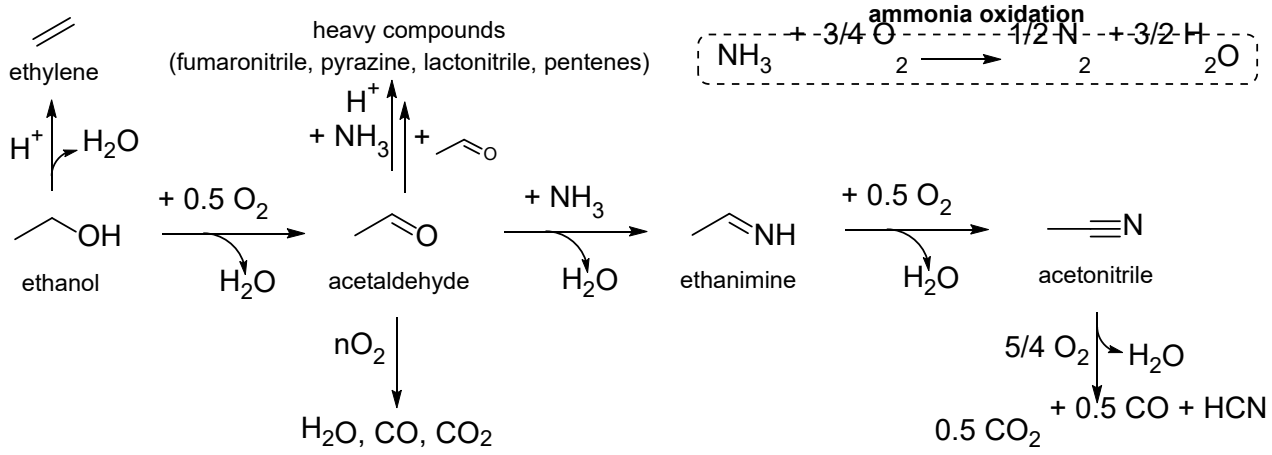

Scheme 2. General reaction network for ethanol ammoxidation to acetonitrile catalyzed by VPP.

3.4 Ethanol ammoxidation: the interaction between VPP and ammonia

To understand the role of the adsorbed ammonia in the reaction mechanism, we conducted some experiments in which we interacted gaseous NH_3 with the VPP catalyst. Martin et al. [33,100] found that during 3-picoline ammoxidation to 3-cyanopyridine, the precursor $VOHPO_4 0.5H_2O$ reacted with gaseous ammonia forming an NH_4-containing V/P/O compound.

Instead, in the case of our VPP, the used catalyst preserved the same structure as the fresh one; however, Raman spectroscopy showed that the used catalyst appeared to be much more reduced than the fresh one, with VPP as the predominant compound and no presence of oxidized $VOPO_4$ compounds (Figure S9), which instead were present in the fresh catalyst.

As shown in Figure S10, TPD/MS experiments conducted by heating the VPP under He flow led to the release of water in the 100 to 200°C temperature interval, but also at temperatures higher than 300°C, and the process was completed at around 450°C. When ammonia was adsorbed on the pre-cleaned VPP catalyst at 100°C, the TPD profile showed only a minimal amount of ammonia desorbed, whereas most of ammonia desorbed in the form of N_2 + H_2O; furthermore, the characterization of the VPP catalyst showed that, after the TPD experiment, the $VOPO_4$ present in the fresh calcined catalyst had disappeared, and only VPP bands were left (Figure S11).

It may be concluded that the chemical interaction of ammonia and VPP is so strong that it is highly unlikely that the acetaldehyde generated *in situ* during ethanol ammoxidation will react with the ammonium ion to generate the imine species, and that the aldehyde may instead be more likely to react with ammonia in the gas phase. This was experimentally demonstrated by first adsorbing ammonia on the VPP catalyst at 100°C, then by recording the IR spectra of the VPP by means of DRIFT spectroscopy at increasing temperatures up to 350°C, and lastly by pulsing ethanol on the catalyst at the latter temperature. The ammonium ion was clearly shown, fully retained even after both increasing the catalyst temperature and pulsing ethanol (Figure S12).

3.5 The oxidation of β-picoline to nicotinic acid: reaction network

The effect of temperature on picoline conversion and selectivity to products is shown in Figure 6. Experiments were conducted by using 1.0 mol% of picoline in air, at a contact time of 2 s. The main reaction products were nicotinic acid (NAc), nicotinaldehyde (NAl), pyridine (PY), cyanopyridine (CP), CO, and CO_2; traces of nicotinamide and bipyridine were also found, however, with a selectivity far lower than 0.2%. Figure 6 shows that the C balance at low temperature was very low, close to 30%, and improved when the temperature was raised, but never

exceeded 70%. NAc maximum yield was only 14% at 310°C; at lower temperatures, NAl also formed, with traces of CO and CO_2, whereas at temperatures higher than 310°C, CO_2 became the predominant product, even though other by-products were formed in considerable amounts (CP, PY, and CO).

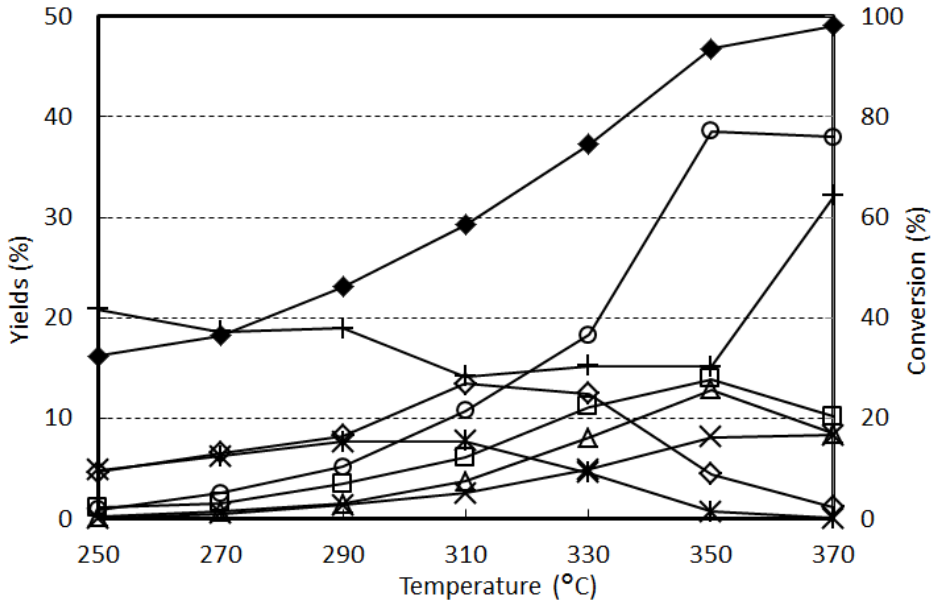

Figure 6. Effect of temperature on β-picoline conversion and yield to products. Reaction conditions: feed composition (molar %): β-picoline/oxygen/inert 1/20/79; contact time 2 s. Symbols: β-picoline conversion (◆), yield to: nicotinic acid (◇), nicotinic aldehyde (✳), pyridine (△), cyanopyridine (□), CO (×), CO_2 (○), and heavy compounds (+). Catalyst VPP.

The formation of heavy compounds, especially at low temperatures, is attributable to the strong adsorptive interaction of reactants and products with the catalyst surface, due to both the high boiling temperature of these compounds and VPP acidity; the protonation of the N atom in the pyridine ring may be responsible for the strong adsorption of the reactant. In fact, an experiment conducted by pulsing pyridine on the VPP catalyst and recording DRIFT spectra during the desorption at increasing temperature (reported in Figure S13), showed that pyridine was retained

up to 400°C, a clear evidence of its strong adsorption in the temperature range used for reactivity experiments.

We repeated the experiment by co-feeding 20 mol% water also; results are plotted in Figure 7. It was seen that the catalytic performance was considerably enhanced in the presence of steam; the best yield to NAc was 36%, again at 310°C, whereas the selectivity to other by-products was similar to that observed in the absence of steam. The most important effect, however, was on C balance, which was close to 100% over the entire range of temperatures investigated, with no formation of heavy compounds. It is also important to note that picoline conversion was greater in the presence of water (for example, at 310°C it was 75%, but only 60% in the absence of water under the same conditions). Overall, water served not only to assist the desorption of NAc while keeping a clean surface and facilitate the interaction between picoline and the active sites, but also to limit the consecutive unselective transformation of NAc or NAl to heavier condensation compounds and accelerate the consecutive oxidation of NAl to NAc. The hydration of NAl and oxidative dehydrogenation of the geminal glycol to NAc may also be one additional reason for the enhanced selectivity to NAc, providing an alternative route to the direct oxidation of NAl; however, at the reaction temperature , carbonyl hydration is thermodynamically disadvantaged.

Figure 8 shows the effect of contact time on catalytic performance (picoline conversion and selectivity to products) for experiments conducted with the co-feeding of H_2O at 310°C; Figure S13 shows the results obtained in the absence of steam.

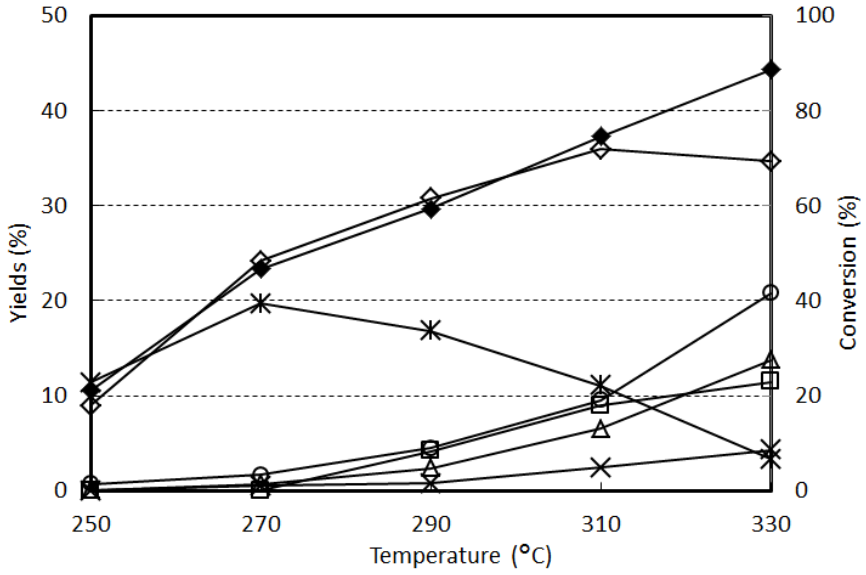

Figure 7. Effect of temperature on β-picoline conversion and yield to products. Reaction conditions: feed composition (molar %): β-picoline/oxygen/steam/inert 1/20/20/59; contact time 2 s. Symbols: β-picoline conversion (◆), yield to: nicotinic acid (◇), nicotinic aldehyde (✳), pyridine (△), cyanopyridine (□), CO (×), and CO_2 (○). Catalyst VPP.

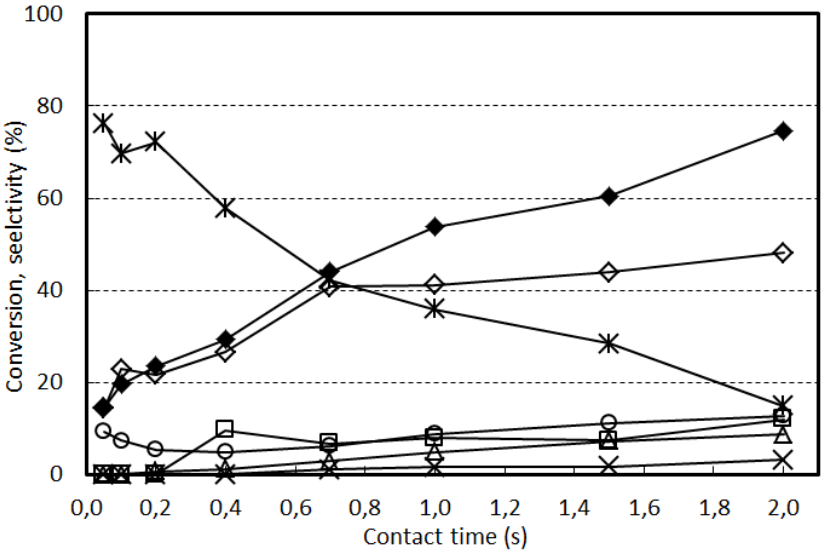

Figure 8. Effect of contact time on β-picoline conversion and selectivity to products. Reaction conditions: feed composition (molar %): β-picoline/oxygen/steam/inert 1/20/20/59; temperature 310°C. Symbols: β-picoline conversion (◆), selectivity to: nicotinic acid NAc (◇), nicotinic aldehyde NAl (✳), pyridine (△), cyanopyridine (□), CO (×), and CO_2 (○). Catalyst VPP.

The kinetic relationship between NAl and NAc is apparent from the experimental results; aldehyde was the main primary product, and its selectivity rapidly declined when the contact time was

increased, with a corresponding increased selectivity to NAc and, to a lesser extent, to other by-products. CO_2 was also a primary product, its selectivity extrapolated to zero contact time being higher than zero. In the case of experiments conducted without steam (Figure S13), some important differences were seen. In this case, the main primary products were heavy compounds (initial C-loss was around 70%) – an event which suggests that (i) at low picoline conversion, the catalyst surface coverage by the adsorbed reactant was very significant, and (ii) under these conditions adsorbed species were transformed mainly into heavy compounds. The increased contact time and picoline conversion led to a progressive decline in the C-loss value, and a corresponding increased selectivity to all products, including NAc. These experiments confirm that, under the given conditions, the saturation of the catalyst surface was responsible for the low selectivity to NAc. This phenomenon may be limited by using a high temperature or contact time; conditions which, however, are more inductive to the formation of by-products derived from oxidative degradation. Conversely, the use of co-fed steam is more efficient and makes it possible to achieve high selectivity to NAc even under relatively milder conditions.

Experiments conducted for ethanol ammoxidation (see above) had also highlighted the importance of limiting saturation effects with the VPP catalyst. Therefore we decided to carry out the reaction under conditions which, in principle, should be more favorable for NAc formation: i.e. a lower molar fraction of picoline and a higher molar fraction of steam in the reactor feed.

Figure 9 shows the effect of temperature with 0.2 mol% picoline and 7% O_2 (in order to keep the same picoline/O_2 ratio as for the experiments in Figure 7), and 67% steam (contact time 1.4 s). Under these conditions, selectivity to NAc was greatly enhanced; a max yield of 55% was obtained at 330°C, with low yields to by-products.

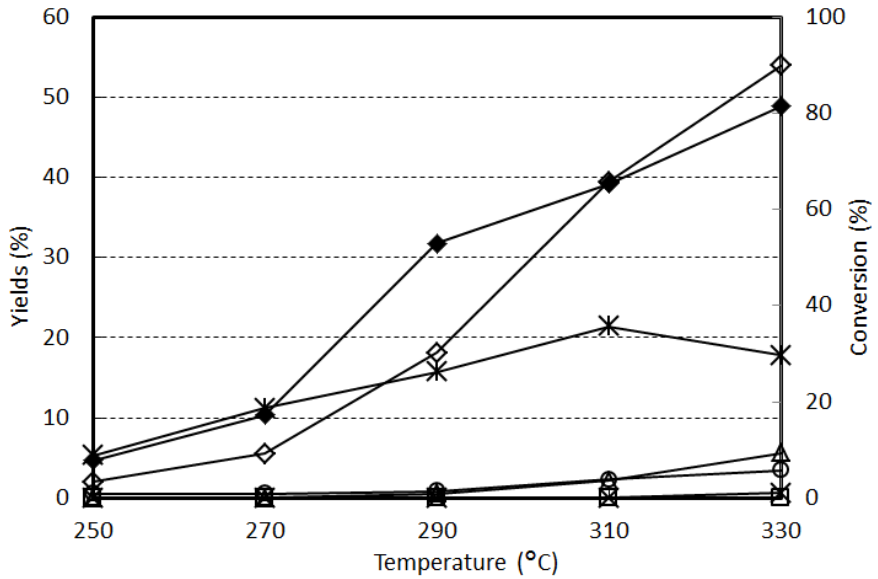

Figure 9. Effect of temperature on β-picoline conversion and yield to products. Reaction conditions: feed composition (molar %): β-picoline/oxygen/steam/inert 0.2/7/67/25.8; contact time 1.4 s. Symbols: β-picoline conversion (◆), yield to: nicotinic acid (◇), nicotinic aldehyde (✳), pyridine (△), cyanopyridine (□), CO (✕), and CO_2 (○). Catalyst VPP.

The experimentally observed max yield to NAc, even under the optimized reaction conditions, is lower than that reported in literature for catalysts based on TiO_2-supported V_2O_5; in this case, yields as high as 90% are reported [83], as summarized in Table S2. The comparatively lower performance of the VPP catalyst is attributable to the poor catalyst efficiency in the consecutive oxidation of NAl into NAc; in fact, Figures 7-9 show that the selectivity to NAl was still relatively high even at high contact time or temperature, when the conversion of picoline was over 60-70%. Instead, with V_2O_5/TiO_2 catalyst, the efficient transformation of the intermediate NAl to NAc leads to an excellent selectivity to the latter compound; with this catalyst type, the selectivity to NAl at high picoline conversion is virtually zero.

This hypothesis was confirmed by experiments conducted by feeding NAl directly; the results are shown in Figure 10 (conditions: 0.2 mol% Nal, O_2 7%, 67% steam, contact time 1.4 s).

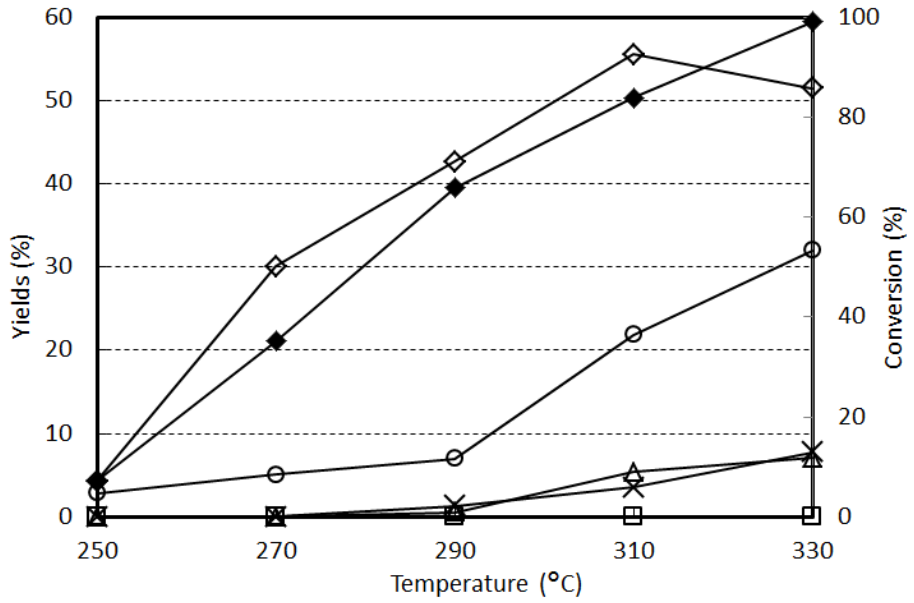

Figure 10. Effect of temperature on nicotinic aldehyde conversion and yield to products. Reaction conditions: feed composition (molar %): NAl/oxygen/steam/inert 0.2/7/67/25.8; contact time 1.4 s. Symbols: nicotinic aldehyde conversion (◆), selectivity to: nicotinic acid (◇), pyridine (△), cyanopyridine (□), CO (×), and CO_2 (○). Catalyst VPP.

It can be seen that the reactivity of the aldehyde was not much different from that of picoline under the same experimental conditions (Figure 9), which is an unexpected result; even though NAc is the prevailing product, considerable yields to CO_2, CO, and pyridine were also observed.

Scheme 3 summarizes the reaction network for 3-picoline oxidation to nicotinic acid with VPP catalyst.

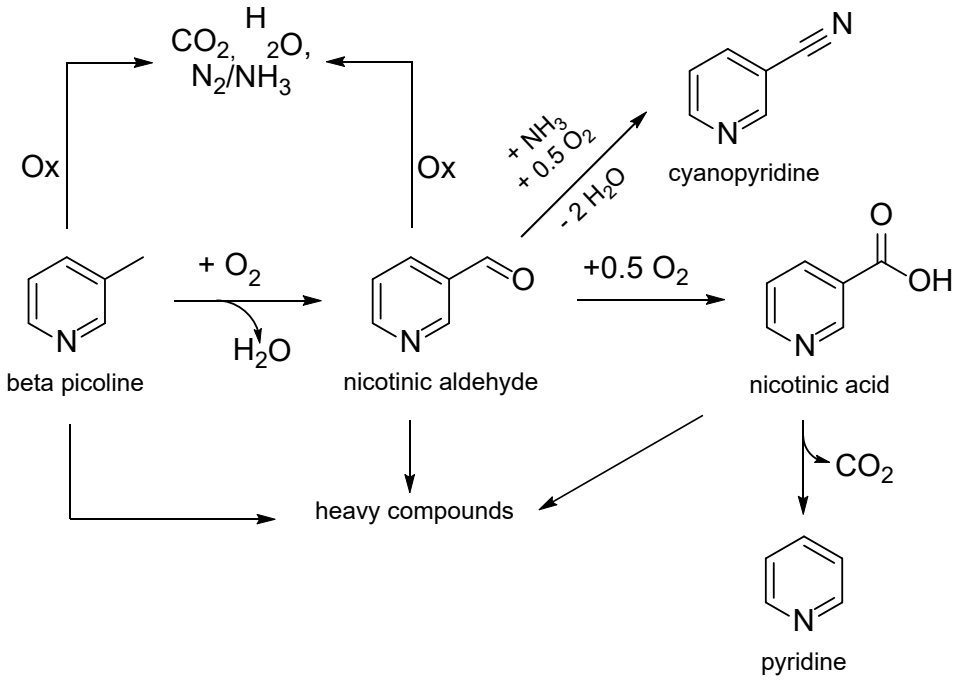

Scheme 3. Reaction network for 3-picoline oxidation to nicotinic acid with VPP catalyst.

After reactivity tests, the catalyst was characterized by means of Raman spectroscopy (Figure S15). Spectra were collected at r.t. by focusing the laser beam over different particles (top Figure); the bands shown correspond to the typical bands of VPP and $VOPO_4$, at 1190, 1135, and 920 cm^{-1} and at 1038, 928, 579, and 541 cm^{-1}, respectively. After reaction at picoline-lean conditions (bottom in Figure S15), spectra showed that the used catalyst particles were not homogeneous. Some particles showed spectra similar to that of fresh VPP, others showed spectra with the typical bands of β-$VOPO_4$ (at 1075, 986, 892, 656, 599, 435, 368, and 284 cm^{-1}). Notably, after reaction in ethanol ammoxidation, the spent catalyst appeared to be completely reduced to $(VO)_2P_2O_7$ (Figure S9). The fresh catalyst ("equilibrated" DuPont VPP) showed the typical bands of both $(VO)_2P_2O_7$ and β/α_I-$VOPO_4$ (Figures S1, S9, and S15)

4. Conclusions: common features and differences in the two reactions investigated

The ammoxidation of ethanol to acetonitrile and the oxidation of β-picoline to nicotinic acid with the VPP catalyst were investigated; the best results achieved are summarized in Table S3. These two reactions share some common features, but there are also differences.

a) In both reactions, the key step is the formation of the aldehyde as the key intermediate, by oxidation of the methyl group in 3-picoline, and by oxidehydrogenation of the alcohol in ethanol ammoxidation. The nature of VPP active phase during *n*-butane oxidation has been investigated by several authors [2,4,7,9,13,14,99]; it has been ascertained that "patches" of V^{5+} compounds develop on the surface of $(VO)_2P_2O_7$, the nature of which depends on both reaction conditions and the P/V atomic ratio in VPP (typically higher than the stoichiometric value of 1.0). In the case of β-picoline oxidation, the reaction conditions used are similar to the typical ones in *n*-butane oxidation, and it may be expected that the nature of the active surface in the two cases is similar. On the other hand, the presence of N atom in picoline may cause a much stronger interaction of the reactant with VPP. Also in the case of ethanol ammoxidation – due to the presence of two reactants, ethanol and ammonia, both of which strongly interact with VPP – and of the higher concentration of reactants, reaction conditions may be considered more reducing than in the case of *n*-butane oxidation.

b) Once the intermediate aldehyde has been formed, it either reacts with NH_3 and eliminates water to form imine (precursor for acetonitrile formation), or is oxidized to nicotinic acid. In the latter case, water plays a fundamental role, as also clearly pointed out in Andrushkevich's papers [83]; it contributes to both picoline activation by Brønsted acid sites generated *in situ* and to the desorption of the acid, thus avoiding its consecutive

combustion. No important role of water is expected in ethanol ammoxidation, because under the reaction conditions used, acetonitrile, a volatile compound, quickly desorbs and does not undergo consecutive combustion reactions, being a relatively more stable compound. On the other hand, the ammonium ion generated by the reaction of VPP is so strongly bound that it remains chemically bound even at the highest reaction temperature and covers the surface, probably contributing to the saturation effect observed in the experiments conducted at increasing reactant partial pressure. Moreover, the ammonium species does not react with ethanol or the intermediately formed acetaldehyde; the intermediate imine is probably formed by reaction between the adsorbed aldehyde and gaseous ammonia.

c) Overall, it seems that the strong acidity of VPP, which is known to play a fundamental role in other reactions, is a burden for the currently investigated reactions, limiting the selectivity to acetonitrile in ethanol ammoxidation because of both the undesired formation of ethylene and the saturation effect due to the strong interaction with reactants. In the case of β-picoline oxidation, the strong interaction between basic reactants and VPP surface is also the reason for the surface saturation effects and the poor selectivity observed in the absence of co-fed steam. Steam helps in facilitating the desorption of products and keeping the VPP surface clean, thus permitting a considerable increase in selectivity.

References

[1] P. Sudarsanam, R. Zhong, S. Van Den Bosch, S.M. Coman, V.I. Parvulescu, B.F. Sels, Chem. Soc. Rev. 47 (2018) 8349–8402.

[2] A. Chieregato, J.M. López Nieto, F. Cavani, Coord. Chem. Rev. 301–302 (2015) 3–23.

[3] C. Bandinelli, B. Lambiase, T. Tabanelli, J. De Maron, N. Dimitratos, F. Basile, P. Concepcion, J.M.L. Nieto, F. Cavani, Appl. Catal. A Gen. 582 (2019) 117102.

[4] A. Caldarelli, M.A. Bañares, C. Cortelli, S. Luciani, F. Cavani, Catal. Sci. Technol. 4 (2014) 419–427.

[5] F. Cavani, J.H. Teles, ChemSusChem 2 (2009) 508–34.

[6] I.E. Wachs, K. Routray, ACS Catal. 2 (2012) 1235–1246.

[7] N. Ballarini, F. Cavani, C. Cortelli, S. Ligi, F. Pierelli, F. Trifirò, C. Fumagalli, G. Mazzoni, T. Monti, Top. Catal. 38 (2006) 147–156.

[8] F. Cavani, N. Ballarini, S. Luciani, Top. Catal. 52 (2009) 935–947.

[9] N.F. Dummer, J.K. Bartley, G.J. Hutchings, Adv. Catal. 54 (2011) 189–247.

[10] D. Lesser, G. Mestl, T. Turek, Appl. Catal. A Gen. 510 (2016) 1–10.

[11] M. Eichelbaum, M. Hävecker, C. Heine, A.M. Wernbacher, F. Rosowski, A. Trunschke, R. Schlögl, Angew. Chem. Int. Ed. Engl. 54 (2015) 2922–6.

[12] A. Shekari, G.S. Patience, Can. J. Chem. Eng. 91 (2013) 291–301.

[13] F. Cavani, D. De Santi, S. Luciani, A. Löfberg, E. Bordes-Richard, C. Cortelli, R. Leanza, Appl. Catal. A Gen. 376 (2010) 66–75.

[14] F. Cavani, S. Luciani, E.D. Esposti, C. Cortelli, R. Leanza, Chemistry 16 (2010) 1646–55.

[15] N. Ballarini, F. Cavani, C. Cortelli, M. Ricotta, F. Rodeghiero, F. Trifirò, C. Fumagalli, G. Mazzoni, Catal. Today 117 (2006) 174–179.

[16] G.J. Hutchings, J. Mater. Chem. 14 (2004) 3385–3395.

[17] M. Dente, S. Pierucci, E. Tronconi, M. Cecchini, F. Ghelfi, Chem. Eng. Sci. 58 (2003) 643–648.

[18] J.T. Cleaves, G. Centi, Catal. Today 16 (1993) 69–78.

[19] G. Centi, Catal. Letters 22 (1993) 53–66.

[20] V.A. Zazhigalov, J. Haber, J. Stoch, B.D. Mikhajluk, A.I. Pyatnitskaya, G.A. Komashko, I. V. Bacherikova, Catal. Letters 37 (1996) 95–99.

[21] F. Cavani, A. Colombo, F. Giuntoli, E. Gobbi, F. Trifirò, P. Vazquez, Catal. Today 32 (1996) 125–132.

[22] F. Cavani, A. Colombo, F. Trifirò, M.T. Sananes Schulz, J.C. Volta, G.J. Hutchings, Catal. Letters 43 (1997) 241–247.

[23] G. Bignardi, F. Cavani, C. Cortelli, T. De Lucia, F. Pierelli, F. Trifirò, G. Mazzoni, C. Fumagalli, T. Monti, J. Mol. Catal. A Chem. 244 (2006) 244–251.

[24] J. Haber, J. Stoch, V.A. Zazhigalov, I. V. Bacherikova, E. V. Cheburakova, Pol. J. Chem. 82 (2008) 1839–1852.

[25] G. Landi, L. Lisi, J.-C. Volta, J. Mol. Catal. A Chem. 222 (2004) 175–181.

[26] G. Landi, L. Lisi, G. Russo, J. Mol. Catal. A Chem. 239 (2005) 172–179.

[27] Y.H. Taufiq-Yap, C.S. Saw, R. Irmawati, Catal. Letters 105 (2005) 103–110.

[28] S. Ieda, S. Phiyanalinmat, S. Komai, T. Hattori, A. Satsuma, J. Catal. 236 (2005) 304–312.

[29] Y. Zhang, A. Martin, H. Berndt, B. Lücke, M. Meisel, J. Mol. Catal. A Chem. 118 (1997) 205–214.

[30] A. Martin, U. Steinike, S. Rabe, B. Lücke, F.K. Hannour, J. Chem. Soc. - Faraday Trans. 93 (1997) 3855–3862.

[31] A. Martin, React. Kinet. Catal. Lett. 60 (1997) 3–8.

[32] A. Martin, L. Wilde, U. Steinike, J. Mater. Chem. 10 (2000) 2368–2374.

[33] A. Martin, C. Janke, V.N. Kalevaru, Appl. Catal. A Gen. 376 (2010) 13–18.

[34] E. Mikolajska, E.R. Garcia, R.L. Medina, A.E. Lewandowska, J.L.G. Fierro, M.A. Bañares, Appl. Catal. A Gen. 404 (2011) 93–102.

[35] P.R. Makgwane, N.I. Harmse, E.E. Ferg, B. Zeelie, Chem. Eng. J. 162 (2010) 341–349.

[36] V. Mahdavi, H.R. Hasheminasab, S. Abdollahi, J. Chinese Chem. Soc. 57 (2010) 189–198.

[37] D.J. Upadhyaya, S.D. Samant, Catal. Today 208 (2013) 60–65.

[38] V. Mahdavi, H.R. Hasheminasab, Appl. Catal. A Gen. 482 (2014) 189–197.

[39] C. Santra, S. Shah, A. Mondal, J.K. Pandey, A.B. Panda, S. Maity, B. Chowdhury, Microporous Mesoporous Mater. 223 (2016) 121–128.

[40] N.P. Rajan, G.S. Rao, B. Putrakumar, K.V.R. Chary, RSC Adv. 4 (2014) 53419–53428.

[41] N. Pethan Rajan, G.S. Rao, V. Pavankumar, K.V.R. Chary, Catal. Sci. Technol. 4 (2014) 81–92.

[42] F. Wang, J.-L. Dubois, W. Ueda, J. Catal. 268 (2009) 260–267.

[43] F. Wang, J.-L. Dubois, W. Ueda, Appl. Catal. A Gen. 376 (2010) 25–32.

[44] J. Deleplanque, J.-L. Dubois, J.-F. Devaux, W. Ueda, Catal. Today 157 (2010) 351–358.

[45] G. Pavarelli, J. Velasquez Ochoa, A. Caldarelli, F. Puzzo, F. Cavani, J.-L. Dubois, ChemSusChem 8 (2015) 2250–9.

[46] G. Busca, G. Centi, F. Trifirò, V. Lorenzelli, J. Phys. Chem. 90 (1986) 1337–1344.

[47] G. Centi, G. Golinelli, F. Trifiro', Appl. Catal. 48 (1989) 13–24.

[48] L.M. Cornaglia, E.A. Lombardo, J.A. Andersen, J.L.G. Fierro, Appl. Catal. A Gen. 100 (1993) 37–50.

[49] A. Martin, U. Bentrup, B. Lücke, A. Brückner, Chem. Commun. (1999) 1169–1170.

[50] A. Brückner, Appl. Catal. A Gen. 200 (2000) 287–297.

[51] K. Aït-Lachgar-Ben Abdelouahad, M. Roullet, M. Brun, A. Burrows, C.. Kiely, J.. Volta, M. Abon, Appl. Catal. A Gen. 210 (2001) 121–136.

[52] I. Sádaba, S. Lima, A.A. Valente, M. López Granados, Carbohydr. Res. 346 (2011) 2785–91.

[53] B.M. Reddy, B. Manohar, J. Chem. Soc. Chem. Commun. (1993) 234–235.

[54] R.R. Rao, N. Srinivas, S.J. Kulkarni, M. Subrahmanyarn, K.V. Raghavan, Indian J. Chem. 36A (1997) 708–711.

[55] A. Martin, V.N. Kalevaru, Q. Smejkal, Catal. Today 157 (2010) 275–279.

[56] B. Lucke, K.V. Narayana, A. Martin, K. Jahnisch, Adv. Synth. Catal. 346 (2004) 1407–1424.

[57] T. Oishi, K. Yamaguchi, N. Mizuno, Top. Catal. 53 (2010) 479–486.

[58] T. Oishi, K. Yamaguchi, N. Mizuno, Angew. Chem. Int. Ed. Engl. 48 (2009) 6286–8.

[59] S.. Kulkarni, R. Ramachandra Rao, M. Subrahmanyam, A. V Rama Rao, J. Chem. Soc. Chem. Commun. (1994) 273.

[60] T. Ishida, H. Watanabe, T. Takei, A. Hamasaki, M. Tokunaga, M. Haruta, Appl. Catal. A Gen. 425–426 (2012) 85–90.

[61] F. Folco, J. Velasquez Ochoa, F. Cavani, L. Ott, M. Janssen, Catal. Sci. Technol. 7 (2017) 200–212.

[62] A. Tripodi, D. Ripamonti, R. Martinazzo, F. Folco, T. Tabanelli, F. Cavani, I. Rossetti, Chem. Eng. Sci. 207 (2019) 862–875.

[63] A. Tripodi, E. Bahadori, D. Cespi, F. Passarini, F. Cavani, T. Tabanelli, I. Rossetti, ACS

Sustain. Chem. Eng. 6 (2018) 5441–5451.

[64] W.F. Hoelderich, Appl. Catal. A Gen. 194–195 (2000) 487–496.

[65] D. Heinz, W.F. Hoelderich, S. Krill, W. Boeck, K. Huthmacher, J. Catal. 192 (2000) 1–10.

[66] E.V. Ovchinnikova, T.V. Andrushkevich, L.A. Shadrina, React. Kinet. Catal. Lett. 82 (2004) 191–197.

[67] G.Y. Popova, Y.A. Chesalov, T.V. Andrushkevich, React. Kinet. Catal. Lett. 83 (2004) 353–360.

[68] R. Chuck, Appl. Catal. A Gen. 280 (2005) 75–82.

[69] G.Y. Popova, T. V. Andrushkevich, I.I. Zakharov, Y.A. Chesalov, Kinet. Catal. 46 (2005) 217–226.

[70] G.Y. Popova, T. V. Andrushkevich, Y.A. Chesalov, E. V. Ovchinnikova, React. Kinet. Catal. Lett. 87 (2006) 387–394.

[71] R. Raja, J.M. Thomas, M. Greenhill-Hooper, S. V Ley, F.A. Almeida Paz, Chemistry 14 (2008) 2340–8.

[72] E. V. Ovchinnikova, T. V. Andrushkevich, React. Kinet. Catal. Lett. 93 (2008) 203–210.

[73] E.Y. Yakovleva, V.Y. Belotserkovskaya, O. V. Skrypnik, J. Anal. Chem. 63 (2008) 863–866.

[74] V.M. Bondareva, E. V. Ovchinnikova, T. V. Andrushkevich, React. Kinet. Catal. Lett. 94 (2009) 327–335.

[75] D. Srinivas, W. Hoelderich, S. Kujath, M. Valkenberg, T. Raja, L. Saikia, R. Hinze, V. Ramaswamy, J. Catal. 259 (2008) 165–173.

[76] G.A. Zenkovets, G.N. Kryukova, S. V. Tsybulya, E.M. Al'kaeva, T. V. Andrushkevich, O.B. Lapina, E.B. Burgina, L.S. Dovlitova, V. V. Malakhov, G.S. Litvak,

Kinet. Catal. 41 (2000) 572–583.

[77] E. V. Ovchinnikova, G.Y. Popova, T. V. Andrushkevich, React. Kinet. Catal. Lett. 96 (2009) 91–100.

[78] E.V. Ovchinnikova, T.V. Andrushkevich, G.Y. Popova, V.D. Meshcheryakov, V.A. Chumachenko, Chem. Eng. J. 154 (2009) 60–68.

[79] E. V. Ovchinnikova, V.A. Chumachenko, N. V. Vernikovskaya, V.N. Kashkin, T. V. Andrushkevich, Russ. J. Appl. Chem. 83 (2010) 846–853.

[80] Y. Tian, B. Zhang, J. Ge, W. Guo, X. Bai, X. Sun, W. Li, Spec. Petrochemicals 27 (2010) 13–16.

[81] Y.A. Chesalov, E.V. Ovchinnikova, G.B. Chernobay, G.Y. Popova, T.V. Andrushkevich, Catal. Today 157 (2010) 39–43.

[82] E.V. Ovchinnikova, N.V. Vernikovskaya, T.V. Andrushkevich, V.A. Chumachenko, Chem. Eng. J. 176–177 (2011) 114–123.

[83] T. V. Andrushkevich, E. V. Ovchinnikova, Catal. Rev. 54 (2012) 399–436.

[84] Y.A. Chesalov, T. V. Andrushkevich, V.I. Sobolev, G.B. Chernobay, J. Mol. Catal. A Chem. 380 (2013) 118–130.

[85] P.B. Vorobyev, L.I. Saurambaeva, T.P. Mikhailovskaya, O.K. Yugay, A.P. Serebryanskaya, I.A. Shlygina, Russ. J. Appl. Chem. 87 (2014) 887–894.

[86] Y. Alkayeva, R. Gibadullin, M. Merakhovich, A. Abdurakhmanov, A. Holubyeva, A. Shutilov, G. Zenkovets, Appl. Catal. A Gen. 491 (2015) 1–7.

[87] E.. Al'kaeva, T.. Andrushkevich, G.. Zenkovets, G.. Kryukova, S.. Tsybulya, Catal. Today 61 (2000) 249–254.

[88] E.M. Al'kaeva, T. V. Andrushkevich, G.A. Zenkovets, G.N. Kryukova, S. V. Tsybulya,

E.B. Burgina, Stud. Surf. Sci. Catal. 110 (1997) 939–946.

[89] R. Chuck, Chimia (Aarau). 54 (2000) 508–513.

[90] S. Zhaoxia, E. Kadowaki, T. Shishido, Y. Wang, K. Takehira, Chem. Lett. (2001) 754–755.

[91] T. Shishido, Z. Song, E. Kadowaki, Y. Wang, K. Takehira, Appl. Catal. A Gen. 239 (2003) 287–296.

[92] N.M. Shaw, K.T. Robins, A. Kiener, Adv. Synth. Catal. 345 (2003) 425–435.

[93] Z. Song, J. Catal. 218 (2003) 32–41.

[94] H.F. Huang, B.C. Zhu, H.F. Lu, H.Y. Liu, Y.F. Chen, Gao Xiao Hua Xue Gong Cheng Xue Bao/Journal Chem. Eng. Chinese Univ. 18 (2004) 334–338.

[95] P. Pollak, G. Romeder, F. Hagedorn, H. Gelbke, Ullmann's Encycl. Ind. Chem. (2005) 1–15.

[96] I.F. McConvey, D. Woods, M. Lewis, Q. Gan, P. Nancarrow, Org. Process Res. Dev. 16 (2012) 612–624.

[97] S. Godbole, M.J. Seely, D. Suresh, Ammoxidation of a Mixture of Alcohols to a Mixture of Nitriles to Acetonitrile and HCN, WO 02/070465A1, 2002.

[98] T. Tatsumi, S. Kunitomi, J. Yoshiwara, A. Muramatsu, H. Tominaga, Catal. Letters 3 (1989) 223–226.

[99] N.F. Dummer, W. Weng, C. Kiely, A.F. Carley, J.K. Bartley, C.J. Kiely, G.J. Hutchings, Appl. Catal. A Gen. 376 (2010) 47–55.

[100] V.N. Kalevaru, N. Madaan, A. Martin, Appl. Catal. A Gen. 391 (2011) 52–62.

Graphical abstract

Bi-functional VPP catalyst for both ethanol ammoxidation to acetonitrile and β-picoline oxidation to nicotinic acid, investigation of reaction mechanisms and the role of acidic and redox sites for the optimization of the selectivity to target products.